

# INTERNATIONAL SOCIETY FOR SOIL MECHANICS AND GEOTECHNICAL ENGINEERING



*This paper was downloaded from the Online Library of the International Society for Soil Mechanics and Geotechnical Engineering (ISSMGE). The library is available here:*

<https://www.issmge.org/publications/online-library>

*This is an open-access database that archives thousands of papers published under the Auspices of the ISSMGE and maintained by the Innovation and Development Committee of ISSMGE.*

## Cyclic Strengths and Simulated CPT Penetration Resistances in Intermediate Soils

A. B. Price<sup>1</sup>, R. W. Boulanger<sup>2</sup>, J. T. DeJong<sup>2</sup>, A. M. Parra Bastidas<sup>3</sup>, D. Moug<sup>3</sup>

### ABSTRACT

An investigation relating laboratory measured cyclic strengths to simulated cone penetration test (CPT) tip resistances in intermediate soils is presented. Crushed, non-plastic silica flour and kaolin clay are blended to create soil mixtures with plasticity indices (PI) of 0, 6, and 20. Undrained cyclic direct simple shear (DSS) testing is performed to characterize the cyclic strength of slurry deposited specimens. Drained and undrained CPT tip resistances are estimated from simulated cavity expansion limit pressures. Cylindrical cavity expansion simulations are performed in the finite difference program FLAC (Itasca 2014) using a modified version of the MIT-S1 elastoplastic constitutive model (Pestana et al. 2002, Jaeger et al. 2012). Leblanc and Randolph's method (2008) for computing CPT tip resistances from cavity limit pressures is used. The addition of a small amount of plasticity (from PI = 0 to 6) is shown to reduce predicted tip resistances by up to a factor of ten while having a much lesser impact on measured cyclic strength. The effect of drainage on simulated CPT tip resistance is shown to produce normalized tip resistance ratios ( $Q_{\text{drained}}/Q_{\text{undrained}}$ ) consistent with experimental values reported in the literature. Results of the simulations and laboratory testing are presented and discussed.

### Introduction

Response of soils during earthquake induced cyclic loading can be roughly partitioned into the categories “sand-like” and “clay-like” based on fundamental differences in the characterization methods most appropriate for sands and clays. Cyclic strength is typically assessed by either semi-empirical triggering curves relating in situ penetration resistance to cyclic strength for sand-like soils or lab testing and strength normalization relationships for clay-like soils. Researchers have suggested different criteria for distinguishing which approach should be adopted for intermediate soils such as sandy silts, sandy clays, and low-plasticity silts. In addition to empirical correlations, researchers have investigated how cyclic strength and cone tip resistance varies across a variety of intermediate soils through cyclic lab testing, calibration chamber cone penetration testing, and numerical simulation of cone penetration (Carraro et al. 2003 Kokusho et al. 2012, Park et al. 2013, Cubrinovski et al. 2010, Salgado et al. 1997, Jaeger et al. 2012). Such work has advanced development of mechanics based frameworks for investigation of the relationships between CPT tip resistance and cyclic strength for intermediate soils.

---

<sup>1</sup>Corresponding Author, Ph. D. Candidate, Department of Civil and Environmental Engineering, University of California, Davis, CA, USA, [abprice@ucdavis.edu](mailto:abprice@ucdavis.edu)

<sup>2</sup>Professor, Department of Civil and Environmental Engineering, University of California, Davis, CA, USA

<sup>3</sup>Ph. D. Candidate, Department of Civil and Environmental Engineering, University of California, Davis, CA, USA

An investigation relating laboratory measured cyclic strengths to simulated CPT tip resistances in intermediate soils is presented. Crushed, non-plastic silica flour (SIL-CO-SIL 250) and kaolin clay (Old Hickory No. 1 Glaze) were blended to create soil mixtures with plasticity indices (PI) of 0, 6, and 20; the PI = 0 mixture was 100% silica flour (referred to as 100S), the PI = 6 mixture was 80% silica flour and 20% kaolin clay by dry mass (80S20K), and the PI = 20 mixture was 30% silica flour and 70% kaolin clay (30S70K). Undrained cyclic direct simple shear (DSS) testing was performed to characterize the cyclic strength of slurry deposited specimens. Monotonic behavior was characterized by monotonic DSS and one dimensional (1D) compression testing. Cylindrical cavity expansion (CCE) simulations were performed in the finite difference program FLAC (Itasca 2014) using a modified version of the MIT-S1 elasto-plastic constitutive model (Pestana et al. 2002, Jaeger et al. 2012). Leblanc and Randolph's method (2008) was used to compute CPT tip resistances from cavity limit pressures. The addition of a small amount of plasticity (from PI 0 to 6) is shown to reduce predicted tip resistance by up to a factor of ten while having a much lesser impact on measured cyclic strength. The effect of drainage on simulated CPT tip resistance is shown to produce normalized tip resistance ratios ( $Q_{\text{drained}}/Q_{\text{undrained}}$ ) consistent with experimental values reported in the literature. The synthesis of lab data and numerical simulations shows promise for mechanistically investigating relationships between cyclic strength and in situ penetration resistance for intermediate soils.

### **MIT-S1 Constitutive Model and Calibration**

The MIT-S1 constitutive model has been shown to be capable of simulating both sand and clay behaviors (Pestana and Whittle 1999, Pestana and Whittle 2002a,b). The model uses the limiting compression curve (LCC) as a key component of its framework. Samples compressed from different initial states are modelled to converge to a single limiting compression curve at high stresses. MIT-S1 is critical state compatible and uses bounding surface plasticity to model the behavior of overconsolidated soils. The critical state line (CSL) has experimentally been shown to parallel the LCC at high stresses providing the basis for unified model (Pestana and Whittle 1999). A slightly modified version of the MIT-S1 constitutive model (Pestana et al. 2002, Jaeger et al. 2012) is used in the present study.

Calibration of the MIT-S1 model for cylindrical cavity expansion simulation and CPT tip resistance estimation was performed to capture the primary behaviors known to affect CPT tip resistance. Undrained tip resistance is most strongly affected by the soil's undrained shear strength, with the shear stiffness and lateral earth pressure having important but secondary effects. Drained tip resistance is most strongly affected by shear strength, volumetric strains, shear stiffness, and lateral earth pressure. Other behaviors such as hysteric responses have tertiary order effects on predicted tip resistance. Therefore, when calibrating MIT-S1 for cavity expansion simulations, priority was given to the simulation of undrained and drained strengths, shear stiffness (from small to large strains), and lateral earth pressures over the range of stresses involved in the simulations. The calibration process involved selecting parameters that control (a) 1D compression behavior, (b) shear modulus and its nonlinearity, (c) lateral earth pressure and its variation with overconsolidation ratio (OCR), (d) the CSL and critical state friction angle, and (e) volumetric swelling and hysteresis. The basis for calibration included 1D compression tests and drained and undrained monotonic DSS testing, supplemented by published correlations for behaviors not captured by the employed testing program.

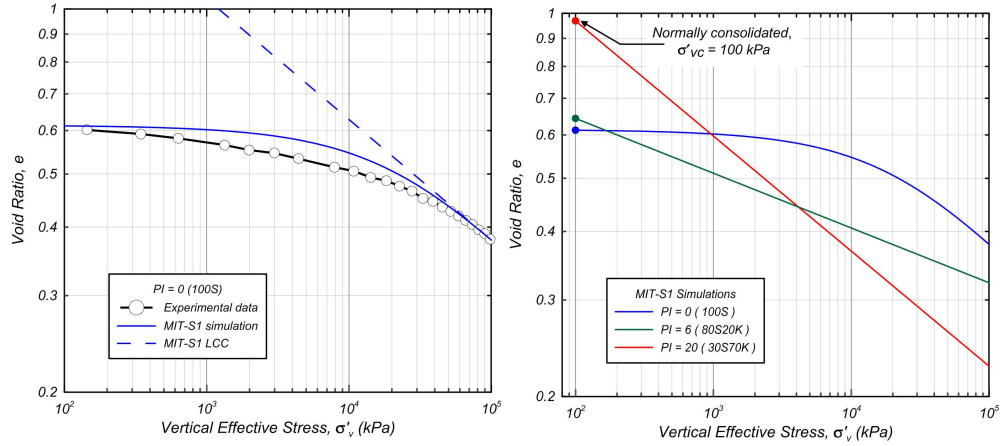


Figure 1. One dimensional compression behavior: (a) experimental and simulated results for PI = 0 mixture, and (b) simulations for PI = 0, 6, 20 mixtures

### Monotonic Loading Responses: Measured and Simulated

Compression behavior was characterized by one dimensional compression testing of slurry deposited specimens to high stresses. MIT-S1 compression behavior is controlled by the elastic modulus, the LCC, and the transitional behavior describing the curvature of the compression curve from low stresses to the LCC regime. The maximum (small strain) elastic modulus was calibrated from Carlton and Pestana's (2012) regression for high and low plasticity clays and silts. The LCC and the curvature of the compression curve were calibrated from experimental compression data. For example, the experimental one dimensional compression curve, the simulated MIT-S1 compression curve and the MIT-S1 LCC for the PI = 0 material are shown in Figure 1a. The one dimensional compression curve merges with the LCC for this PI = 0 mixture at a vertical effective stress ( $\sigma'_v$ ) greater than about 40 MPa. The simulated compression behaviors for all three mixtures are shown in Figure 1b, along with their initial states when normally consolidated to  $\sigma'_v = 100$  kPa. The PI = 0 mixture was much less compressible than the other mixtures for  $\sigma'_v$  up to 10 to 20 MPa, which encompasses the range of stresses involved in the cavity expansion simulations presented later. The PI = 20 mixture has a much higher void ratio for  $\sigma'_v$  less than about 1 MPa and is much more compressible than the other two mixtures. For the PI = 6 and 20 mixtures, their LCC and compression curves are the same, which is common for slurry sedimented clays.

Shearing behavior was characterized by drained and undrained monotonic DSS testing of slurry deposited specimens consolidated to a vertical effective consolidation stress ( $\sigma'_{vc}$ ) ranging from 100 kPa to 1,600 kPa, and overconsolidation ratios (OCR) ranging from 1 to 8. Experimental and simulated stress-strain curves for normally consolidated (NC) specimens of the three mixtures are shown in Figure 2. The PI = 6 and 20 mixtures show undrained shear strength normalization over the stress range tested ( $\sigma'_{vc}$  of 100 to 800 kPa) with undrained shear strength ratios of  $s_u/\sigma'_{vc} = 0.16$  and 0.2, respectively. The critical state lines for these mixtures were parallel to their LCCs, as expected. The PI = 0 soil was dilative at large shear strains over the stress range tested ( $\sigma'_{vc}$  of 100 to 1600 kPa). Parameters controlling the volumetric strain during one dimensional

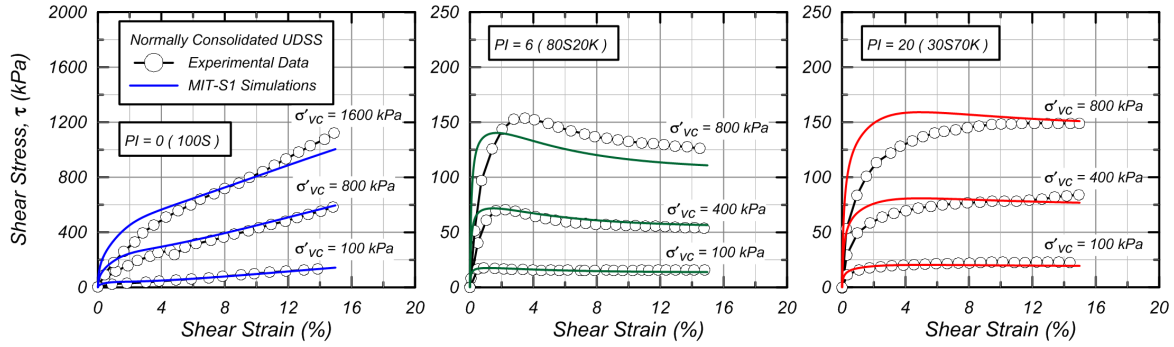


Figure 2. Monotonic undrained DSS test results and simulations:  
(a) PI = 0 (b) PI = 6, and (c) PI = 20

unloading were calibrated to the measured variation of undrained shear strength with overconsolidation ratio. Shear modulus degradation was calibrated to produce undrained stress paths consistent with experimental results while remaining within the bounds of expected shear modulus reduction behavior.

### Measured Cyclic Strengths

Cyclic strengths were characterized by stress controlled undrained cyclic DSS testing. The cyclic strengths for specimens consolidated at  $\sigma'_{vc}$  of 100 kPa with OCRs of 1 and 4 are summarized in Figure 3a showing the combinations of cyclic stress ratio (CSR) and number of uniform loading cycles required to reach 3% shear strain (single amplitude). The cyclic resistance ratio (CRR) for failure defined as 3% shear strain in 15 cycles is plotted versus OCR in Figure 3b. The trend lines on this figure are based on the CRR varying with OCR raised to an exponent value; exponents of 0.45, 0.62, and 0.54 were used to generate the fits for the PI = 0, 6, and 20 mixtures, respectively. The CRR values ranged from 0.10 to 0.14 for the NC specimens, with the PI = 6 mixture having the lowest CRR value. The CRR values ranged from about 0.21 to 0.29 at OCR = 4, being roughly twice the values for the NC specimens. An empirical curve for sedimentary clays based on a normalized undrained shear strength ratio of  $s_u/\sigma'_{vc} = S \cdot \text{OCR}^m$  with  $S = 0.22$  and  $m = 0.8$  and a cyclic strength ratio of  $(\tau_{cyc}/s_u)_{N=15 \text{ cycles}} = 0.92$  is also shown on Figure 3b for comparison. The CRR values from this empirical relationship are greater than obtained for the PI = 6 and 20 mixtures, which may partly reflect the young age of the laboratory specimens.

The addition of clay to non-plastic soil has been shown to increase the contractive tendency and reduce strength during undrained shearing (Prakasha and Chandrasekaran 2005, Bouferra and Shahrour 2004). For constant void ratio silt-clay mixtures, Guo and Prakash (1999) summarized that cyclic strength decreases with addition of plastic fines for PI < 5 and increases for PI > 10. The monotonic and cyclic experimental results obtained in this study show qualitative agreement with these observations.

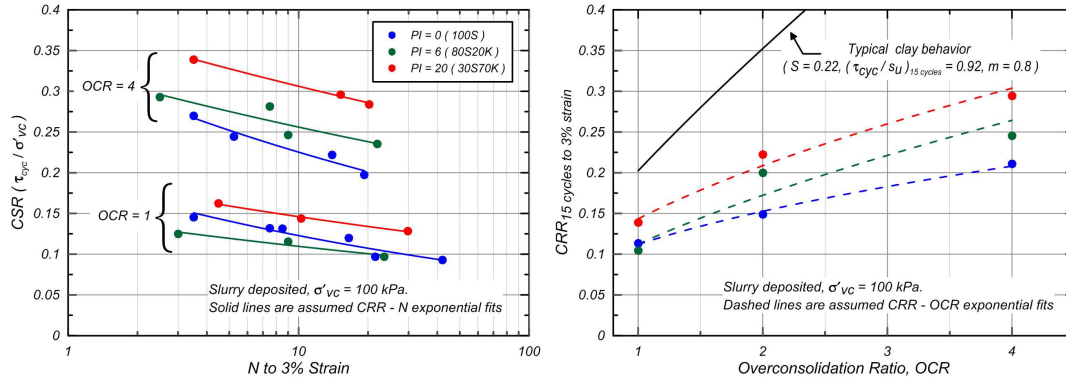


Figure 3. Cyclic DSS test results: (a) CSR vs number of cycles, (b) CRR versus OCR

### Simulated Penetration Resistance

Cylindrical cavity expansion simulations were performed using the finite-difference platform FLAC (Itasca 2014) with the calibrated MIT-S1 constitutive model. The FLAC model used is described in detail by Jaeger et al. (2012). Expansion is simulated using 100 axisymmetric zones with the nodal spacing suggested by Yu (1994). The cavity is expanded from an initial radius,  $a_0$ , to a radius 10 times the initial radius. The initial cavity radius was set equal to the cone penetrometer radius (2.2 cm) divided by  $\sqrt{3}$  as suggested by Silva et al. (2006) and used by Jaeger et al. (2012). Radial extents of 10 m and much larger were used in sensitivity analyses to confirm there were no boundary effects. Zero vertical displacement boundary conditions were used at all nodes and force boundary conditions were used at the radial extent of the model to simulate the initial lateral earth pressure as illustrated in Figure 4.

CPT tip resistances were estimated from the CCE simulation results following Leblanc and Randolph (2008). The projection of stresses from the cavity expansion simulations onto the cone face are illustrated in Figure 4. The cavity limit pressure, taken to be the effective radial stress acting at the cavity wall at an expansion ratio,  $a/a_0$ , of 10, is assumed to be the minor principal stress acting radially on the entire cone face. The interface friction angle between the cone face and surrounding soil,  $\delta$ , is assumed to be the triaxial compression critical state friction angle of the soil. The vertical effective stress acting on the cone face is assumed to be the major principal stress and can be solved for given the cone geometry. This interpretation was applied to both sands and clays, although it is recognized that this approach does not account well for dilatancy during drained penetration (e.g., by comparison to the method of Yu 1994).

Simulated tip resistances for both drained and undrained conditions are shown for OCR values of 1, 2, and 4 in Figure 5. The PI = 6 and 20 mixtures have much lower (almost an order of magnitude lower) penetration resistances than the PI = 0 material at all OCR values. The lower penetration resistances for the plastic mixtures is consistent with them exhibiting greater compressibility (Figure 1b) and lower undrained shear strengths (Figure 2) than the PI = 0 material. An empirical relationship between tip resistance and OCR in clays based on normalized undrained shear strengths ( $S = 0.22$  and  $m = 0.8$ ) with a cone bearing factor of  $N_{kt} = 15$  gives slightly greater undrained penetration resistances than simulated for the PI = 6 and 20 mixtures, which is partly attributed to the young age of these sedimented specimens. Ratios of drained to

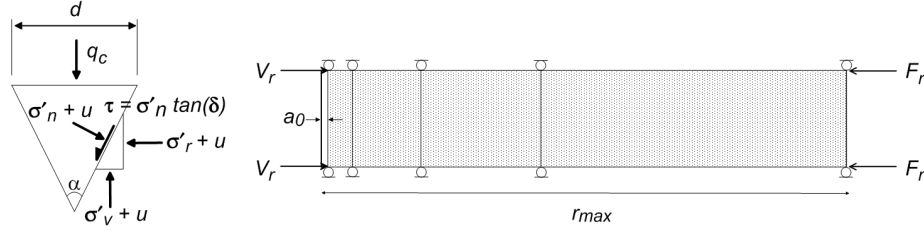


Figure 4. Cylindrical cavity expansion boundary conditions and stress projection onto cone face

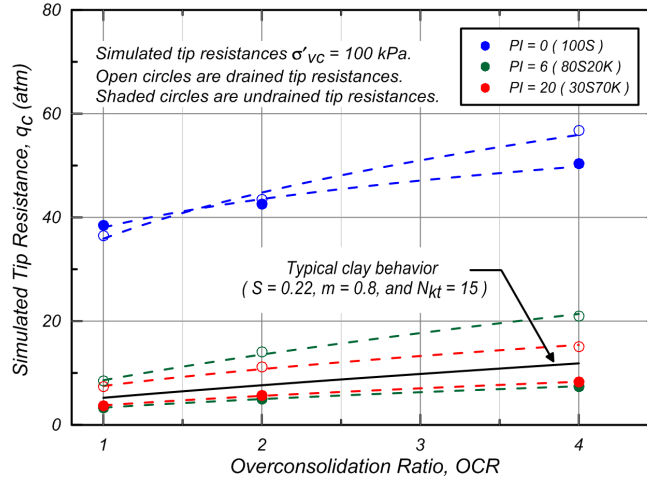


Figure 5. Simulated tip resistance vs. OCR

undrained tip resistances for the  $PI = 6$  and  $20$  mixtures range from about 2 to 3, which are consistent with experimental results for clays summarized in DeJong and Randolph (2012). The  $PI = 0$  material has similar drained and undrained simulated tip resistances, which is attributed to the dilative tendency of this material over the range of initial states covered by these simulations.

### Relating CRR and $q_c$

The laboratory measured cyclic strengths are related to the simulated CPT tip resistances in Figure 6 for all three mixtures and  $\sigma'_{vc} = 100$  kPa. The shaded regions for each mixture indicate the range of tip resistances for drained and undrained conditions. CPT penetration in the field would be expected to range from partially drained for the  $PI = 0$  and  $6$  mixtures to largely undrained for the  $PI = 20$  material, based on their measured coefficients of consolidation and established relationships for drainage during cone penetration (e.g., DeJong and Randolph 2012). The curves relating CRR to tip resistance for the  $PI = 6$  and  $20$  mixtures are located much further to the left than the curves for the  $PI = 0$  material. This leftward shift with a small amount of plasticity is primarily due to the order-of-magnitude smaller tip resistances for the  $PI = 6$  and  $20$  mixtures, whereas the CRR values for all three mixtures at any given OCR varied to a lesser extent. This result is consistent with studies showing that the leftward shift in SPT liquefaction triggering correlations with increasing fines content is largely attributable to the effects of the fines on the SPT penetration resistance (e.g., Cubrinovski et al. 2010).

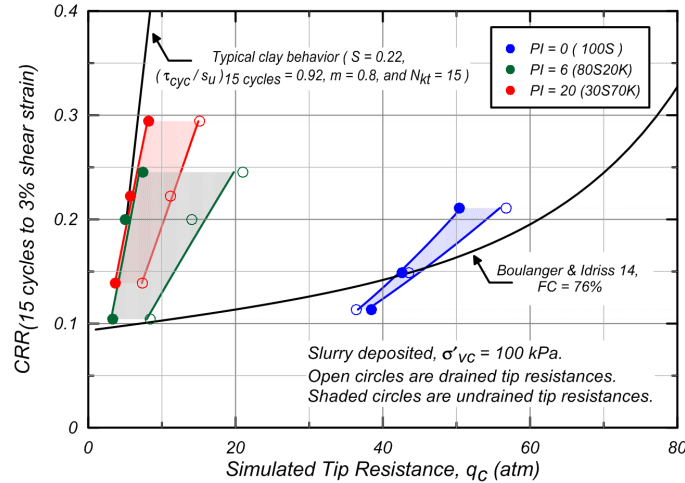


Figure 6. Measured cyclic strength vs simulated CPT tip resistance

Empirical curves of CRR versus tip resistance are also shown on Figure 6 for clays and nonplastic silts at a  $\sigma'_{vc}$  of 100 kPa. The empirical curve for clays is based on  $S = 0.22$ ,  $m = 0.8$ ,  $(\tau_{cyc}/s_u)_{N=15 \text{ cycles}} = 0.92$ , and  $N_{kt} = 15$ . The empirical curve for nonplastic silts is the CPT based liquefaction correlation by Boulanger and Idriss (2014) for a fines content of 76% (i.e., the fines content of the  $PI = 0$  material). The relationships between CRR and undrained tip resistance for the  $PI = 6$  and 20 mixtures are in reasonable agreement with the empirical curve for ordinary sedimentary clays. The range of CRR versus tip resistance curves for the  $PI = 0$  material is also in reasonable agreement with its corresponding empirical correlation for nonplastic liquefiable soils (Boulanger and Idriss 2014). The reasonable agreement between the relationships developed for these  $PI = 0$ , 6, and 20 mixtures and their applicable empirical counterparts is promising in suggesting that the present approach can be used to further examine the use of CPT tests for estimating cyclic strengths of intermediate soils across a broader range of in-situ conditions.

## Conclusions

Laboratory measured cyclic strengths have been related to simulated CPT tip resistances for three mixtures of silica flour and kaolin clay ( $PI = 0, 6, 20$ ). Cyclic strengths were characterized by undrained DSS testing at overconsolidation ratios ranging from 1 to 4. CPT tip resistance was estimated by cylindrical cavity expansion simulation in FLAC using the modified MIT-S1 constitutive model and projecting the cavity limit pressure onto the cone face following LeBlond and Randolph (2008). The addition of a small amount of plasticity (from  $PI = 0$  to 6) was shown to reduce simulated tip resistances by about an order of magnitude while having a much lesser impact on measured cyclic strength. The synthesis of lab data and numerical simulation shows promise for mechanistically investigating relationships between cyclic strength and in situ penetration resistance for intermediate soils over a broader range of conditions.

## Acknowledgments

Portions of the work presented herein were derived from studies supported by the California Department of Water Resources (DWR) and the National Science Foundation (grants CMMI-1138203 and CMMI-1300518). Any opinions, findings, or recommendations expressed in this

material are those of the authors and should not be interpreted as necessarily representing the official policies, either expressed or implied, of either organization.

## References

- Bouferra, R., and Shahrou, I. (2004). "Influence of fines on the resistance to liquefaction of a clayey sand." *Proceedings of the ICE - Ground Improvement*, **8**(1), 1-5.
- Boulanger, R. W., and Idriss, I. M. (2014). "CPT and SPT based liquefaction triggering procedures." Report No. UCD/CGM-14/01, Center for Geotechnical Modeling, University of California, Davis, CA, 134 pp.
- Carlton, B. D., and Pestana, J. M. (2012). "Small strain shear modulus of high and low plasticity clays and silts." *15th World conference on earthquake engineering*, Lisbon, Portugal.
- Carraro, J. A. H., Bandini, P., and Salgado, R. (2003). "Liquefaction Resistance of Clean and Nonplastic Silty Sands Based on Cone Penetration Resistance." *J. Geotechnical and Geoenvironmental Engineering*, **129**(11), 965-976.
- Cubrinovski, M., Rees, S., and Bowman, E. (2010). "Effects of Non-plastic Fines on Liquefaction Resistance of Sandy Soils." 17, 125-144.
- DeJong, J. T., and Randolph, M. (2012). "Influence of Partial Consolidation during Cone Penetration on Estimated Soil Behavior Type and Pore Pressure Dissipation Measurements." *JGGE, ASCE*, **138**(7), 777-788.
- Guo, T., and Prakash, S. (1999). "Liquefaction of Silts and Silt-Clay Mixtures." *Journal of Geotechnical and Geoenvironmental Engineering*, **125**(8), 706-710.
- Jaeger, R. A. (2012). "Numerical and experimental study of cone penetration in sands and intermediate soils." Doctoral dissertation, University of California, Davis.
- Kokusho, T., Ito, F., Nagao, Y., and Green, A. R. (2012). "Influence of Non/Low-Plastic Fines and Associated Aging Effects on Liquefaction Resistance." *J. Geotechnical and Geoenvironmental Engineering*, **138**(6), 747-756.
- LeBlanc, C., and Randolph, M. F. (2008). "Interpretation of piezocones in silt, using cavity expansion and critical state methods." *Proc. 12th International Conference of IACMAG*, 822-829.
- Park, S.-S., and Kim, Y.-S. (2013). "Liquefaction Resistance of Sands Containing Plastic Fines with Different Plasticity." *Journal of Geotechnical and Geoenvironmental Engineering*, **139**(5), 825-830.
- Pestana, J. M., and Whittle, A. J. (1999). "Formulation of a unified constitutive model for clays and sands." *Int. J. Numer. Anal. Meth. Geomech*, **23**, 1215-1243.
- Pestana, J. M., Whittle, A. J., and Salvati, L. A. (2002a). "Evaluation of a constitutive model for clays and sands: Part I - sand behaviour." *Intnl. J. for Numerical and Analytical Methods in Geomechanics*, **26**(11), 1097-1121.
- Pestana, J. M., Whittle, A. J., and Gens, A. (2002b). "Evaluation of a constitutive model for clays and sands: Part II - clay behaviour." *Intnl. Journal for Numerical and Analytical Methods in Geomechanics*, **26**(11), 1123-1146.
- Prakasha, K. S., and Chandrasekaran, V. S. (2005). "Behavior of Marine Sand-Clay Mixtures under Static and Cyclic Triaxial Shear." *Journal of Geotechnical and Geoenvironmental Engineering*, **131**(2), 213-222.
- Salgado, R., Mitchell, J. K., and Jamiolkowski, M. (1997). "Cavity Expansion and Penetration Resistance in Sand." *Journal of Geotechnical and Geoenvironmental Engineering*, **123**(4), 344-354.
- Silva, M. F., White, D. J., and Bolton, M. D. (2006). "An analytical study of the effect of penetration rate on piezocone tests in clay." *International Journal for Numerical and Analytical Methods in Geomechanics*, **30**(6), 501-527.
- Yu, H. S. (1994). "State Parameter from Self-Boring Pressuremeter Tests in Sand." *Journal of Geotechnical Engineering*, **120**(12), 2118-2135.